HHS Public Access

Author manuscript

Biochem Biophys Res Commun. Author manuscript; available in PMC 2021 September 10.

Published in final edited form as:

Biochem Biophys Res Commun. 2020 September 10; 530(1): 107–114. doi:10.1016/j.bbrc.2020.07.031.

AAV9-*DOK7* Gene Therapy Reduces Disease Severity in *Smn*$^{2B/-}$ SMA Model Mice

Kevin A. Kaifer[1,2], **Eric Villalón**[1,2], **Caley E. Smith**[1,2], **Madeline E. Simon**[1,2], **Jose Marquez**[1,2], **Abigail E. Hopkins**[1,2], **Toni I. Morcos**[1,2], **Christian L. Lorson**[1,2,*]

[1]Department of Veterinary Pathobiology, College of Veterinary Medicine, University of Missouri, Columbia, Missouri, USA.

[2]Bond Life Sciences Center, University of Missouri, Columbia, MO, 65211

Abstract

Spinal Muscular Atrophy (SMA) is an autosomal recessive neuromuscular disease caused by deletions or mutations in the *survival motor neuron* (*SMN1)* gene. An important hallmark of disease progression is the pathology of neuromuscular junctions (NMJs). Affected NMJs in the SMA context exhibit delayed maturation, impaired synaptic transmission, and loss of contact between motor neurons and skeletal muscle. Protection and maintenance of NMJs remains a focal point of therapeutic strategies to treat SMA, and the recent implication of the NMJ-organizer Agrin in SMA pathology suggests additional NMJ organizing molecules may contribute. *DOK7* is an NMJ organizer that functions downstream of Agrin. The potential of *DOK7* as a putative therapeutic target was demonstrated by adeno-associated virus (AAV)-mediated gene therapy delivery of *DOK7* in Amyotrophic Lateral Sclerosis (ALS) and Emery Dreyefuss Muscular Dystrophy (EDMD). To assess the potential of *DOK7* as a disease modifier of SMA, we administered AAV-*DOK7* to an intermediate mouse model of SMA. AAV9-*DOK7* treatment conferred improvements in NMJ architecture and reduced muscle fiber atrophy. Additionally, these improvements resulted in a subtle reduction in phenotypic severity, evidenced by improved grip strength and an extension in survival. These findings reveal *DOK7* is a novel modifier of SMA.

[*]To whom correspondence should be addressed: Christian L. Lorson, Department of Veterinary Pathobiology, Christopher S. Bond Life Sciences Center, 1201 Rollins, Room 471G, University of Missouri, Columbia, MO 65211-7310, USA Tel: +1 573 884 2219, Fax: +1 573 884 9395, orsonc@missouri.edu.

Author Contributions

Experiments were planned by K.A.K. and C.L.L. and performed by K.A.K. and E.V. Data analyses were conducted by C.E.S., M.E.S., J.M., T.I.M. and A.E.H. This manuscript was prepared by K.A.K. and C.L.L.

Competing Interests

C.L.L. is the co-founder and Chief Scientific Officer of Shift Pharmaceuticals.

DOK7 can reduce disease severity in a mouse model of Spinal Muscular Atrophy

DOK7 functions independently of SMN

Provides mechanistic insight into disease relevant pathways and potential novel therapeutic targets

Introduction

Spinal Muscular Atrophy (SMA) is a devastating neurodegenerative disease and a leading genetic cause of infant mortality with a worldwide incidence of 1 in 10,000 live births[1]. Without early medical intervention, most individuals with severe SMA die by two years of age and experience progressive atrophy of skeletal muscle and degeneration of alpha motor neurons[2]. SMA arises from insufficient levels of Survival Motor Neuron (SMN) protein, an essential and ubiquitously expressed housekeeping protein that functions in a variety of RNA metabolism pathways [3,4]. Increasing SMN has proven to be the most effective therapeutic strategy and the recent approval of two breakthrough SMN-inducing modalities, Spinraza and Zolgensma, has transformed the clinical landscape of this disease[5,6]. However, the specific molecular mechanisms of degeneration in SMA are still being elucidated in order to identify additional therapeutic targets for future therapies to address the breadth of the disease, non-responsive patients, and to expand the therapeutic window. These "SMN-independent" modalities have aimed to be either neuroprotective or muscle activating[7,8]. In SMA, impairments in neuromuscular junctions (NMJs) include delayed maturation, reduced quantal release, decreased endplate area, and denervation[9,10]. Additionally, these defects can precede other motor neuron pathologies such as axonal degeneration and motor neuron death[11]. Thus, therapeutic correction of NMJ pathology could prevent motor neuron degeneration and preserve aspects of muscle function. This warrants further characterization of the mechanisms underlying NMJ degeneration.

Several lines of evidence suggest NMJ defects in SMA are influenced by dysfunction in the Agrin/MuSK signaling pathway, which is essential for the development, maturation, and maintenance of NMJs[12]. Agrin, a motor neuron-derived proteoglycan that reinforces acetylcholine receptor (AChR) clustering at the endplate of developing NMJs, is mis-spliced in motor neurons of SMA mice[13]. Agrin transcripts in SMA mice exhibit the aberrant exclusion of exons 32–33, or "Z-exons", which are essential for the AChR clustering property of Agrin[14]. Overexpression of Z^+ Agrin increases NMJ innervation and size, reduces muscle fiber atrophy, and extends survival in SMNΔ7 SMA mice[15]. Phenotypic improvements in SMNΔ7 mice were also observed following administration of the Agrin biological NT-1654, further confirming the importance of Agrin to the pathogenic mechanism of SMA [16].

Modification by Z^+ Agrin implicates a novel set of putative molecular targets for SMA, as Agrin's post-synaptic receptor complex, Lrp4 and MuSK, signal through multiple downstream factors[17–19]. One such factor, downstream of tyrosine kinases 7 (*DOK7*), has recently gained attention as a protective modifier of several neuromuscular diseases[20,21]. *DOK7* is a noncatalytic scaffold protein that is essential for NMJ development, functioning in the activation of MuSK and also in signal transduction following stimulation of MuSK by Agrin[22]. The importance of *DOK7* is emphasized by the observation that mice lacking *DOK7* fail to develop NMJs and that mutations in *DOK7* are associated with Limb Girdle Myasthenia[23–26]. Conversely, overexpression of *DOK7* enlarges NMJs and provides a significant therapeutic benefit in Emery Dreyefuss Muscular Dystrophy (EDMD) and Amyotrophic Lateral Sclerosis (ALS)[20,21,27]. Administration of AAV9-*DOK7* in the *hSOD1-G93A* mouse model of ALS increased endplate area and improved innervation of

affected NMJs, suggesting that *DOK7* elicits retrograde signals that influence both pre- and post-synaptic properties of NMJs[21]. Taken together, these *DOK7* activities suggest a potential modifying role in the SMA context through enlargement of NMJs. To test this hypothesis, we employed AAV9-mediated gene delivery of *DOK7* in the *Smn*$^{2B/-}$ intermediate mouse model of SMA.

Results

We and others have previously shown that, compared to severe models of SMA, the slightly milder *Smn*$^{2B/-}$ or pharmacologically-induced intermediate models are better-suited for the characterization of SMN-independent modalities[28–36]. Here, we utilize the *Smn*$^{2B/-}$ mouse model in the congenic C57BL/6J background[37,38]. Although these mice are ambulatory, they possess important hallmarks of SMA disease pathology including NMJ defects, skeletal muscle atrophy, loss of motor neuron soma, and a predictably early mortality. These characteristics make the *Smn*$^{2B/-}$ mouse a useful experimental system to assess the protective effects of *DOK7* gene therapy. We constructed a self-complementary AAV9 (scAAV9) vector expressing *DOK7* from the constitutive chicken beta-actin promoter to express *DOK7* in *Smn*$^{2B/-}$ mice. scAAV9-*DOK7* was administered intravenously on postnatal day 1 (P1) at a dose of 1×10^{11} vector genomes per mouse, a dose we have previously used in a variety of SMA contexts [31,39,40]. *DOK7* protein levels were increased in hindlimb skeletal muscle following treatment, confirming that administration of the scAAV9-DOK7 vector induced robust upregulation of *DOK7* in the target tissue (Fig 1a). Conceptually, since we were proposing that DOK7 functioned independently of Smn, it was also important to demonstrate that scAAV9-*DOK7* treatment did not significantly increase SMN expression, which was confirmed by western blot (Fig 1b).

Smn$^{2B/-}$ untreated mice lived an average of 21.2 ± 2 days, and we found that scAAV9-*DOK7* prevented early deaths and induced a subtle, but statistically significant, extension in mean survival to 22.2 ± 2 days (Fig. 1C). These results are consistent with the recent report that repletion of Z^+ Agrin in motor neurons of severe SMNΔ7 mice also extends survival[15,16]. scAAV9-*DOK7*-treated mice did not exhibit a significant increase in weight gain compared to *Smn*$^{2B/-}$ untreated mice (Fig. 1d), consistent with other SMN-independent strategies that extended survival, but did not impact total body weight [31,40]. To determine if treatment resulted in a functional improvement in motor activity, we employed a four-limb grip strength assay. scAAV9-*DOK7* significantly improved grip strength at mid-stage disease progression compared to untreated SMA littermates and improvement was more pronounced at disease end stage (Fig. 1e). Taken together, these results demonstrate that modulation of Agrin/MuSK signaling through scAAV9-*DOK7* treatment promotes modest gross phenotypic improvements, suggesting that pathogenic signaling events at affected NMJs are partially corrected.

SMA patients and mouse models exhibit denervation and reduction in motor endplate area of NMJs in a subset of skeletal muscles, resulting in a loss of connectivity in neuromuscular synaptic transmission that significantly contributes to disease pathology [9,10,41]. Because overexpression of *DOK7* has been shown to increase endplate area through enhanced recruitment of AChR clustering, we assessed whether scAAV9-*DOK7* treatment can

suppress reduction of endplate area in SMA. In the *Smn*$^{2B/-}$ mouse model, the NMJs at the transverse abdominis (TVA) muscle are vulnerable to degeneration[11]. We assessed the impact of scAAV9-*DOK7* on NMJs of the TVA muscle by performing immunohistochemical staining on P17, mid-symptomatic disease stage. scAAV9-*DOK7* treatment prevented the reduction in endplate area compared to untreated *Smn*$^{2B/-}$ mice, and also significantly increased endplate area compared to unaffected *Smn*$^{2B/+}$ controls (Fig. 2a,b). To assess whether this activity confers presynaptic improvements in NMJs, we quantified the percentage of fully, partially, and denervated endplates. scAAV9-*DOK7* treatment did not increase the average percentage of innervated endplates compared to untreated *Smn*$^{2B/-}$ mice (Fig. 2c,d). These results suggest that *DOK7* improves pre- and post-synaptic aspects of degenerating NMJs in motor neuron diseases[20,21].

Due to the observed improvements in NMJ pathology, we hypothesized that *DOK7* may reduce motor neuron degeneration. Although motor neuron cell death and NMJ pathology are believed to be regulated by separate processes, delivery of muscle-enhancing factors has previously been shown to increase the number motor neuron soma in the ventral horn of SMA mice[42–44]. Towards this end, we examined the L4-L6 spinal cord at P21, a late symptomatic time point, using immunohistochemistry (Fig. 3a). As expected, untreated *Smn*$^{2B/-}$ mice exhibited a significant loss of motor neuron soma compared to unaffected *Smn*$^{2B/+}$ mice, while the average count of L4-L6 soma in scAAV9-*DOK7*-treated mice was between the unaffected and SMA counts, however, neither comparison was statistically significant (Figure 3b). scAAV9-*DOK7* did not increase motor neuron soma size, as there was no increase in soma area or perimeter compared to *Smn*$^{2B/-}$ mice (Fig. 3c). These results suggest scAAV9-*DOK7* does not improve central defects.

The loss of contact between motor neurons and skeletal muscle contributes to the atrophy of muscle fibers in SMA. Improvements in NMJ pathology following scAAV9-*DOK7* gene therapy suggest that treatment also reduces the impact of skeletal muscle atrophy. To test this hypothesis, we focused our analysis on the tibialis anterior (TA) and soleus (SO) muscles, which consist predominantly of fast twitch and slow twitch fibers, respectively. Cross sectional analysis of both fibers reveals significant reduction in muscle fiber area in the untreated SMA cohort compared to the unaffected littermates. scAAV9-*DOK7* significantly improved muscle fiber area of TA and SO muscles compared to the untreated *Smn*$^{2B/-}$ mice (Fig. 4a,b). These results, together with the functional improvement in motor activity, support a muscle protective role of *DOK7* in SMA.

Discussion

Recent advances in SMA therapy have brought promise to the SMA community, as two highly-efficacious therapies have been approved: Spinraza, an *SMN2*-splice switching antisense oligonucleotide; and Zolgensma, an scAAV9-mediated gene therapy of the SMN coding sequence, which has applied for FDA approval following success in clinical trials[6]. With these breakthrough therapies, early therapeutic intervention can lessen the impact of disease severity for patients of the entire clinical spectrum of SMA. As the long-term requirements for an optimal therapeutic regimen remain to be fully determined, additional consideration must be given to SMA patients that are initiated on therapy post-

symptomatically[45–47]. Investigation of the molecular mechanisms underlying SMA has revealed the high degree of complexity associated with degeneration, and that an increasing number of putative therapeutic targets modify disease severity[48]. This warrants further identification and characterization of novel, disease-modifying therapeutic targets.

Following recent reports that modulation of Agrin-MuSK signaling reduces severity in SMA mice, our findings suggest that the MuSK-activating protein *DOK7* is a novel protective modifier of SMA. Treatment with scAAV9-*DOK7* confers subtle benefits on the phenotype of intermediate *Smn*$^{2B/-}$ SMA mice, evidenced by modest extension in survival, increased weight gain, and improved grip strength. We identified several histological improvements that likely explain the improvements in overall phenotype. scAAV9-*DOK7* treatment in *Smn*$^{2B/-}$ mice dramatically increases NMJ endplate area of NMJs of compared to both untreated *Smn*$^{2B/-}$ mice and unaffected controls, consistent with the known function of *DOK7* in AChR clustering.

There are distinctions to be made between our results and those following repletion of Z^+ Agrin in SMA mice. Although both factors act in the same signaling pathway, overexpression of Z^+ Agrin did not increase endplate area above that of wild type controls, unlike scAAV9-*DOK7*[15]. This can be attributed to differing roles of *DOK7* and Agrin, in which *DOK7* functions both to activate MuSK prior to Agrin signaling and also to propagate the MuSK signal following Agrin signaling. Thus, our results suggest that targeting of muscle-derived factors involved in NMJ organization, such as *DOK7*, might be better-suited to attain enlargement of motor endplates than the motor neuron-derived Agrin.

Our results contribute to the growing body of evidence that *DOK7* is a potential therapeutic target that can be utilized to treat a panel of neuromuscular diseases. In the case of SMA, *DOK7* could be targeted in combination with highly efficacious, SMN-inducing therapies to enhance the integrity of affected NMJs. Towards this aim, characterization of the electrophysiological impact of *DOK7* upregulation in SMA is necessary to determine if the observed histological improvements correlate with functional improvements in synaptic transmission. Finally, *DOK7*-mediated therapy represents a putative strategy for prolonging the therapeutic window SMA treatment and it should be assessed whether *DOK7*-mediated therapy enhances the functionality of NMJs upon post-symptomatic administration.

Materials and Methods

Animal procedures and delivery of therapeutics

All animal experiments and conditions were approved by the Institutional Animal Care and Use Committee (IACUC) at the University of Missouri (protocol #9091).

Smn$^{2B/-}$ mice of the C57/BL6 background were a gift from Dr. Rashmi Kothary at the University of Ottawa, Canada. Animals of both sexes were used in all experiments. Treatment groups were assigned at random. Genotyping was performed by PCR assay following tail biopsy on P0. 1×10^{11} vector genomes of scAAV9-DOK7 were administered systemically via intravenous (IV) injection using the superficial vein on postnatal day 1. Grip-strength assays were conducted by placing all limbs on grid and giving mice two trials,

one for training and the second for data collection (BioSeb Model BP32025, Vitrolles). Mice were fed low-fat stock diets (Harlan Teklad 8640).

Production and purification of scAAV9-DOK7 vector

scAAV9-DOK7 was constructed via triple transfection of Rep2Cap9 (a gift from James Wilson, University of Pennsylvania, Philadelphia, PA), pHelper, and scAAV-CBA-*DOK7* in HEK 293T (ATCC® CRL-3216™) cells using 25-kDa polyethyleneimine. Virus purification and quantification were performed following previously used protocols[49,50].

Histological analysis and quantification of skeletal muscle fiber area

Four animals from both control cohorts and the scAAV9-*DOK7*-treated cohort were randomly selected and harvested at P17. Tibialis anterior (TA) and soleus (SO) muscles were dissected and flash frozen in O.C.T. media (Tissue-Tek) using liquid nitrogen-cooled isopentane. Frozen muscle was cryosectioned at 18 μm per section. Muscle fibers were labeled using anti-laminin primary antibody (1:300; catalog L9393, Sigma) and Alexa Flour 647-conjugated Donkey anti-Rabbit (1:200; Catalog AP187SA6, EMD Millipore) secondary antibody. Samples were mounted using Citiflour AFI mounting media (Ted Pella, Inc.). Imaging was performed using a laser scanning confocal microscope (20X objective; Leica TCS SP8, Leica Microsystems, Inc.). Samples were blinded and approximately 200 muscle fibers were analyzed using ImageJ software (NIH). Individual muscle fibers were pooled across mice per treatment condition. Statistical analysis was performed using a one-way ANOVA with Tukey's multiple comparisons test[51].

Immunohistochemistry of motor neuron soma

Three animals from each treatment group were randomly selected at P21, euthanized, and perfused in 4% Formaldehyde in PBS. The L4-L6 region was dissected, cross sectioned, and stained with ChAT (1:100; catalog AB144P; MilliporeSigma) and NeuroTrace Nissl (Thermo Fisher). Representative images were taken using a laser scanning confocal microscope (20X objective; Leica TCS SP8, Leica Microsystems, Inc.). Motor neuron counts and soma area were quantified using ImageJ software (NIH)[51].

Immunohistochemistry of Neuromuscular Junctions

Four animals from *Smn*$^{2B/+}$ and seven from untreated and scAAV9-*DOK7* treated *Smn*$^{2B/-}$ cohort were randomly selected and harvested at P17. Transverse abdominus muscles were dissected and fixed in 4% Formaldehyde in PBS. Muscles were stained using anti-neurofilament-heavy (1:4000; catalog CPCA-NF-L, EnCore) and anti-synaptophysin (1:200; catalog YE269, Life Technologies™) primary antibodies, and Alexa Flour 488-conjugated Donkey anti-Chicken (1:400; EMD Millipore) and Donkey anti-Rabbit (1:200; EMD Millipore) secondary antibodies. Acetylcholine receptors were labeled with Alexa Flour 594-conjugated α-bungarotoxin (Life Technologies™). Muscles were whole mounted using Citiflour AF1 mounting media (Ted Pella, Inc.). NMJ analysis was performed on 4 randomly selected fields of view per mouse (20X objective; Leica DM5500 B, Leica Microsystems Inc.). Endplate area was measured using ImageJ software (NIH). Representative images

were taken using a laser scanning confocal microscope (20X objective; Leica TCS SP8, Leica Microsystems, Inc.)[51].

Immunoblot

Hindlimb skeletal muscles were harvested at P17. Tissues were lysed using JLB buffer [50 mM Tris pH=8.0, 150 mM NaCl, 10% Glycerol, 20 mM NaH_2PO_4, 50 mM NaF, 2mM EDTA, 5 mM $NaVO_3$] supplied with cOmplete™, Mini Protease Inhibitor Cocktail (Roche). Following SDS-PAGE, protein was transferred to Immobilon®-P transfer membrane (MilliporeSigma) and probed with the following primary antibodies: anti-SMN (1:10,000; 610647, BD Transduction Laboratories™), anti-Calnexin (1:2000; catalog C4731, Sigma), anti-DOK7 (A-7) (1:1000; catalog sc-390856, Santa Cruz Biotechnology). Horseradish peroxidase-conjugated secondary antibodies were used (Jackson ImmunoResearch Laboratories). Immunoblots were visualized using (BioSpectrum® 815 Imaging System, UVP, LLC)[51].

Acknowledgements

This work was supported by funding from NIH (R21NS106490 (C.L.L.)). CES is supported by NIH Training Grant (T32 GM008396) and JM is supported by NIH PREP (R25GM064120).

References

1. Sugarman EA et al. Pan-ethnic carrier screening and prenatal diagnosis for spinal muscular atrophy: clinical laboratory analysis of >72,400 specimens. European journal of human genetics : EJHG 20, 27–32, doi:10.1038/ejhg.2011.134 (2012). [PubMed: 21811307]
2. Crawford TO & Pardo CA The neurobiology of childhood spinal muscular atrophy. Neurobiology of disease 3, 97–110, doi:10.1006/nbdi.1996.0010 (1996). [PubMed: 9173917]
3. Coady TH & Lorson CL SMN in spinal muscular atrophy and snRNP biogenesis. Wiley interdisciplinary reviews. RNA 2, 546–564, doi:10.1002/wrna.76 (2011). [PubMed: 21957043]
4. Fallini C, Bassell GJ & Rossoll W Spinal muscular atrophy: the role of SMN in axonal mRNA regulation. Brain research 1462, 81–92, doi:10.1016/j.brainres.2012.01.044 (2012). [PubMed: 22330725]
5. Hoy SM Nusinersen: A Review in 5q Spinal Muscular Atrophy. CNS Drugs 32, 689–696, doi:10.1007/s40263-018-0545-1 (2018). [PubMed: 30027400]
6. Sumner CJ & Crawford TO Two breakthrough gene-targeted treatments for spinal muscular atrophy: challenges remain. J Clin Invest 128, 3219–3227, doi:10.1172/jci121658 (2018). [PubMed: 29985170]
7. Bordet T, Berna P, Abitbol JL & Pruss RM Olesoxime (TRO19622): A Novel Mitochondrial-Targeted Neuroprotective Compound. Pharmaceuticals (Basel) 3, 345–368, doi:10.3390/ph3020345 (2010). [PubMed: 27713255]
8. Hwee DT et al. The small-molecule fast skeletal troponin activator, CK-2127107, improves exercise tolerance in a rat model of heart failure. J Pharmacol Exp Ther 353, 159–168, doi:10.1124/jpet.114.222224 (2015). [PubMed: 25678535]
9. Kong L et al. Impaired synaptic vesicle release and immaturity of neuromuscular junctions in spinal muscular atrophy mice. The Journal of neuroscience : the official journal of the Society for Neuroscience 29, 842–851, doi:29/3/842 [pii] 10.1523/JNEUROSCI.4434-08.2009 (2009). [PubMed: 19158308]
10. Kariya S et al. Reduced SMN protein impairs maturation of the neuromuscular junctions in mouse models of spinal muscular atrophy. Human molecular genetics 17, 2552–2569, doi:10.1093/hmg/ddn156 (2008). [PubMed: 18492800]

11. Murray LM et al. Selective vulnerability of motor neurons and dissociation of pre- and post-synaptic pathology at the neuromuscular junction in mouse models of spinal muscular atrophy. Human molecular genetics 17, 949–962, doi:10.1093/hmg/ddm367 (2008). [PubMed: 18065780]
12. Misgeld T, Kummer TT, Lichtman JW & Sanes JR Agrin promotes synaptic differentiation by counteracting an inhibitory effect of neurotransmitter. Proc Natl Acad Sci U S A 102, 11088–11093, doi:10.1073/pnas.0504806102 (2005). [PubMed: 16043708]
13. Zhang Z et al. Dysregulation of synaptogenesis genes antecedes motor neuron pathology in spinal muscular atrophy. Proc Natl Acad Sci U S A 110, 19348–19353, doi:10.1073/pnas.1319280110 (2013). [PubMed: 24191055]
14. Burgess RW, Nguyen QT, Son YJ, Lichtman JW & Sanes JR Alternatively spliced isoforms of nerve- and muscle-derived agrin: their roles at the neuromuscular junction. Neuron 23, 33–44 (1999). [PubMed: 10402191]
15. Kim JK, Caine C, Awano T, Herbst R & Monani UR Motor neuronal repletion of the NMJ organizer, Agrin, modulates the severity of the spinal muscular atrophy disease phenotype in model mice. Hum Mol Genet 26, 2377–2385, doi:10.1093/hmg/ddx124 (2017). [PubMed: 28379354]
16. Boido M et al. Increasing Agrin Function Antagonizes Muscle Atrophy and Motor Impairment in Spinal Muscular Atrophy. Front Cell Neurosci 12, 17, doi:10.3389/fncel.2018.00017 (2018). [PubMed: 29440993]
17. Li L, Xiong WC & Mei L Neuromuscular Junction Formation, Aging, and Disorders. Annu Rev Physiol 80, 159–188, doi:10.1146/annurev-physiol-022516-034255 (2018). [PubMed: 29195055]
18. Hallock PT, Chin S, Blais S, Neubert TA & Glass DJ Sorbs1 and −2 Interact with CrkL and Are Required for Acetylcholine Receptor Cluster Formation. Mol Cell Biol 36, 262–270, doi:10.1128/mcb.00775-15 (2016). [PubMed: 26527617]
19. Hallock PT et al. Dok-7 regulates neuromuscular synapse formation by recruiting Crk and Crk-L. Genes Dev 24, 2451–2461, doi:10.1101/gad.1977710 (2010). [PubMed: 21041412]
20. Arimura S et al. Neuromuscular disease. DOK7 gene therapy benefits mouse models of diseases characterized by defects in the neuromuscular junction. Science 345, 1505–1508, doi:10.1126/science.1250744 (2014). [PubMed: 25237101]
21. Miyoshi S et al. DOK7 gene therapy enhances motor activity and life span in ALS model mice. EMBO Mol Med 9, 880–889, doi:10.15252/emmm.201607298 (2017). [PubMed: 28490573]
22. Bergamin E, Hallock PT, Burden SJ & Hubbard SR The cytoplasmic adaptor protein Dok7 activates the receptor tyrosine kinase MuSK via dimerization. Mol Cell 39, 100–109, doi:10.1016/j.molcel.2010.06.007 (2010). [PubMed: 20603078]
23. Okada K et al. The muscle protein Dok-7 is essential for neuromuscular synaptogenesis. Science 312, 1802–1805, doi:10.1126/science.1127142 (2006). [PubMed: 16794080]
24. Beeson D et al. Dok-7 mutations underlie a neuromuscular junction synaptopathy. Science 313, 1975–1978, doi:10.1126/science.1130837 (2006). [PubMed: 16917026]
25. Muller JS et al. Phenotypical spectrum of DOK7 mutations in congenital myasthenic syndromes. Brain 130, 1497–1506, doi:10.1093/brain/awm068 (2007). [PubMed: 17439981]
26. Palace J et al. Clinical features of the DOK7 neuromuscular junction synaptopathy. Brain 130, 1507–1515, doi:10.1093/brain/awm072 (2007). [PubMed: 17452375]
27. Inoue A et al. Dok-7 activates the muscle receptor kinase MuSK and shapes synapse formation. Sci Signal 2, ra7, doi:10.1126/scisignal.2000113 (2009). [PubMed: 19244212]
28. Kaifer KA et al. Plastin-3 extends survival and reduces severity in mouse models of spinal muscular atrophy. JCI Insight 2, doi:10.1172/jci.insight.89970 (2017).
29. Hosseinibarkooie S et al. The Power of Human Protective Modifiers: PLS3 and CORO1C Unravel Impaired Endocytosis in Spinal Muscular Atrophy and Rescue SMA Phenotype. Am J Hum Genet 99, 647–665, doi:10.1016/j.ajhg.2016.07.014 (2016). [PubMed: 27499521]
30. Feng Z et al. Pharmacologically induced mouse model of adult spinal muscular atrophy to evaluate effectiveness of therapeutics after disease onset. Hum Mol Genet 25, 964–975, doi:10.1093/hmg/ddv629 (2016). [PubMed: 26758873]

31. Villalon E et al. AAV9-Stathmin1 gene delivery improves disease phenotype in an intermediate mouse model of spinal muscular atrophy. Human molecular genetics 28, 3742–3754, doi:10.1093/hmg/ddz188 (2019). [PubMed: 31363739]
32. Torres-Benito L et al. NCALD Antisense Oligonucleotide Therapy in Addition to Nusinersen further Ameliorates Spinal Muscular Atrophy in Mice. American journal of human genetics 105, 221–230, doi:10.1016/j.ajhg.2019.05.008 (2019). [PubMed: 31230718]
33. Rimer M et al. Nerve sprouting capacity in a pharmacologically induced mouse model of spinal muscular atrophy. Scientific reports 9, 7799, doi:10.1038/s41598-019-44222-2 (2019). [PubMed: 31127156]
34. Strathmann EA et al. Evaluation of potential effects of Plastin 3 overexpression and low-dose SMN-antisense oligonucleotides on putative biomarkers in spinal muscular atrophy mice. PloS one 13, e0203398, doi:10.1371/journal.pone.0203398 (2018). [PubMed: 30188931]
35. Janzen E et al. CHP1 reduction ameliorates spinal muscular atrophy pathology by restoring calcineurin activity and endocytosis. Brain : a journal of neurology 141, 2343–2361, doi:10.1093/brain/awy167 (2018). [PubMed: 29961886]
36. Bowerman M et al. Therapeutic strategies for spinal muscular atrophy: SMN and beyond. Disease models & mechanisms 10, 943–954, doi:10.1242/dmm.030148 (2017). [PubMed: 28768735]
37. Eshraghi M, McFall E, Gibeault S & Kothary R Effect of genetic background on the phenotype of theSmn2B/−mouse model of spinal muscular atrophy. Human Molecular Genetics, ddw278, doi:10.1093/hmg/ddw278 (2016).
38. Bowerman M, Murray LM, Boyer JG, Anderson CL & Kothary R Fasudil improves survival and promotes skeletal muscle development in a mouse model of spinal muscular atrophy. BMC medicine 10, 24, doi:10.1186/1741-7015-10-24 (2012). [PubMed: 22397316]
39. Shababi M et al. Partial restoration of cardio-vascular defects in a rescued severe model of spinal muscular atrophy. Journal of molecular and cellular cardiology 52, 1074–1082, doi:10.1016/j.yjmcc.2012.01.005 (2012). [PubMed: 22285962]
40. Kaifer KA et al. Plastin-3 extends survival and reduces severity in mouse models of spinal muscular atrophy. JCI Insight 2, e89970, doi:10.1172/jci.insight.89970 (2017). [PubMed: 28289706]
41. Martinez-Hernandez R et al. Synaptic defects in type I spinal muscular atrophy in human development. The Journal of pathology 229, 49–61, doi:10.1002/path.4080 (2013). [PubMed: 22847626]
42. Rose FF Jr., Mattis VB, Rindt H & Lorson CL Delivery of recombinant follistatin lessens disease severity in a mouse model of spinal muscular atrophy. Human molecular genetics 18, 997–1005, doi:10.1093/hmg/ddn426 (2009). [PubMed: 19074460]
43. Zhou H et al. Myostatin inhibition in combination with antisense oligonucleotide therapy improves outcomes in spinal muscular atrophy. J Cachexia Sarcopenia Muscle 11, 768–782, doi:10.1002/jcsm.12542 (2020). [PubMed: 32031328]
44. Biondi O et al. IGF-1R Reduction Triggers Neuroprotective Signaling Pathways in Spinal Muscular Atrophy Mice. The Journal of neuroscience : the official journal of the Society for Neuroscience 35, 12063–12079, doi:10.1523/JNEUROSCI.0608-15.2015 (2015). [PubMed: 26311784]
45. Robbins KL, Glascock JJ, Osman EY, Miller MR & Lorson CL Defining the therapeutic window in a severe animal model of spinal muscular atrophy. Hum Mol Genet, doi:10.1093/hmg/ddu169 (2014).
46. Foust KD et al. Intravascular AAV9 preferentially targets neonatal neurons and adult astrocytes. Nature biotechnology 27, 59–65, doi:nbt.1515[pii]10.1038/nbt.1515 (2009).
47. Mendell JR et al. Single-Dose Gene-Replacement Therapy for Spinal Muscular Atrophy. N Engl J Med 377, 1713–1722, doi:10.1056/NEJMoa1706198 (2017). [PubMed: 29091557]
48. Hosseinibarkooie S, Schneider S & Wirth B Advances in understanding the role of disease-associated proteins in spinal muscular atrophy. Expert Rev Proteomics 14, 581–592, doi:10.1080/14789450.2017.1345631 (2017). [PubMed: 28635376]

49. Mayginnes JP et al. Quantitation of encapsidated recombinant adeno-associated virus DNA in crude cell lysates and tissue culture medium by quantitative, real-time PCR. Journal of virological methods 137, 193–204, doi:10.1016/j.jviromet.2006.06.011 (2006). [PubMed: 16860883]

50. Kaifer KA et al. AAV9-Mediated Delivery of miR-23a Reduces Disease Severity in Smn2B-/SMA Model Mice. Hum Mol Genet, doi:10.1093/hmg/ddz142 (2019).

51. Kaifer KA et al. AAV9-mediated delivery of miR-23a reduces disease severity in Smn2B/−SMA model mice. Human molecular genetics 28, 3199–3210, doi:10.1093/hmg/ddz142 (2019). [PubMed: 31211843]

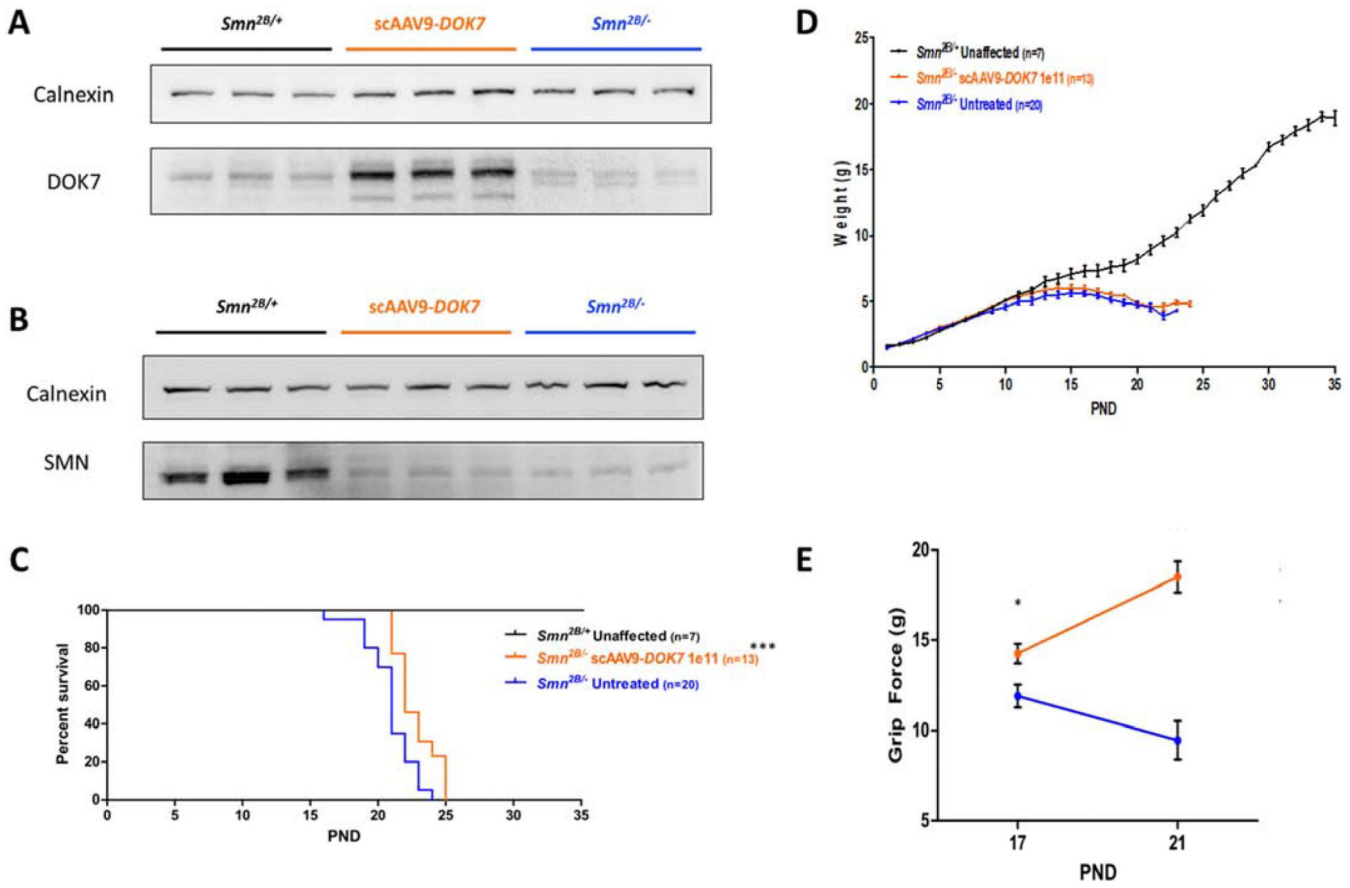

Figure 1: scAAV9-*DOK7* improves phenotype of *Smn*$^{2B/-}$ mice.

(**A**) Western blot of DOK7 in hindlimb skeletal muscle. (**B**) Western blot of SMN in hindlimb skeletal muscle. (**C**) Kaplan-Meier curve of *Smn*$^{2B/-}$ mice treated with scAAV9-*DOK7*. Difference between scAAV9-*DOK7*-treated and untreated *Smn*$^{2B/-}$ mice was calculated using log-rank Mantel-Cox test (**D**) Weight gain of *Smn*$^{2B/-}$ mice treated with scAAV9-*DOK7*. (**E**) Average grip strength on P17 and P21. Groups were compared using Student's t-test. (*P<0.05, ***P<0.001)

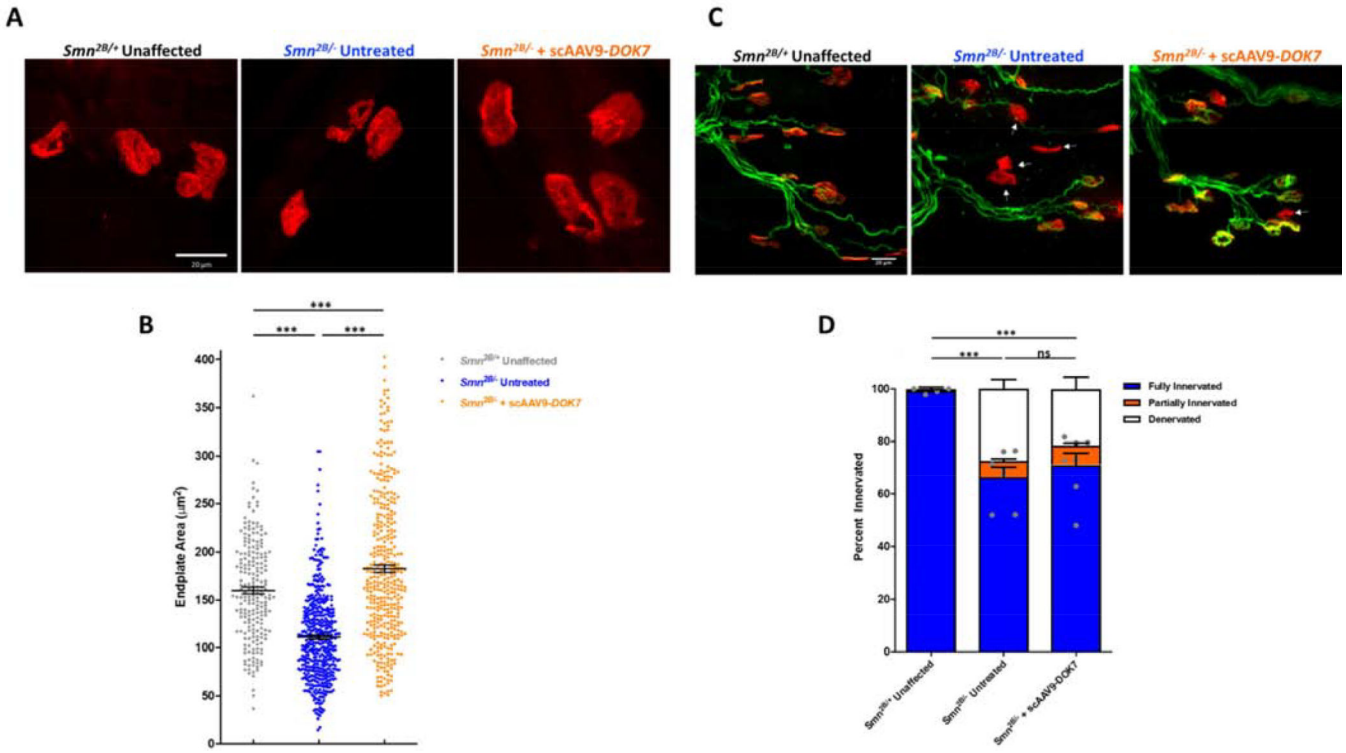

Figure 2: scAAV9-*DOK7* improves endplate area of NMJs in *Smn*$^{2B/-}$ mice.

Transverse abdominus muscles were dissected from mice harvested on P17. (**A**) Representative images of neuromuscular junction endplates labelled with α-bungarotoxin (red). Images were taken with 40X objective lens (scale bars = 20 μm). (**B**) Scatter plot representing quantification of motor endplate area. Bars represent mean ± SEM. (**C**) Representative images of neuromuscular junctions stained with neurofilament (green) and synaptophysin (green) to label the presynaptic terminals and α-bungarotoxin (red) to label endplates. (**D**) Bar graph representing average percentage of fully innervated, partially innervated, and denervated motor endplates. Bars represent mean ± SEM. Statistical analysis was performed comparing degree of fully-innervated endplates. Experimental groups were compared using one-way ANOVA with Tukey's multiple comparisons test. (*Smn*$^{2B/+}$ n=4; *Smn*$^{2B/-}$ n=7; *Smn*$^{2B/-}$ + scAAV9-DOK7 n=7) (***$P < 0.001$, $^{ns}P > 0.05$)

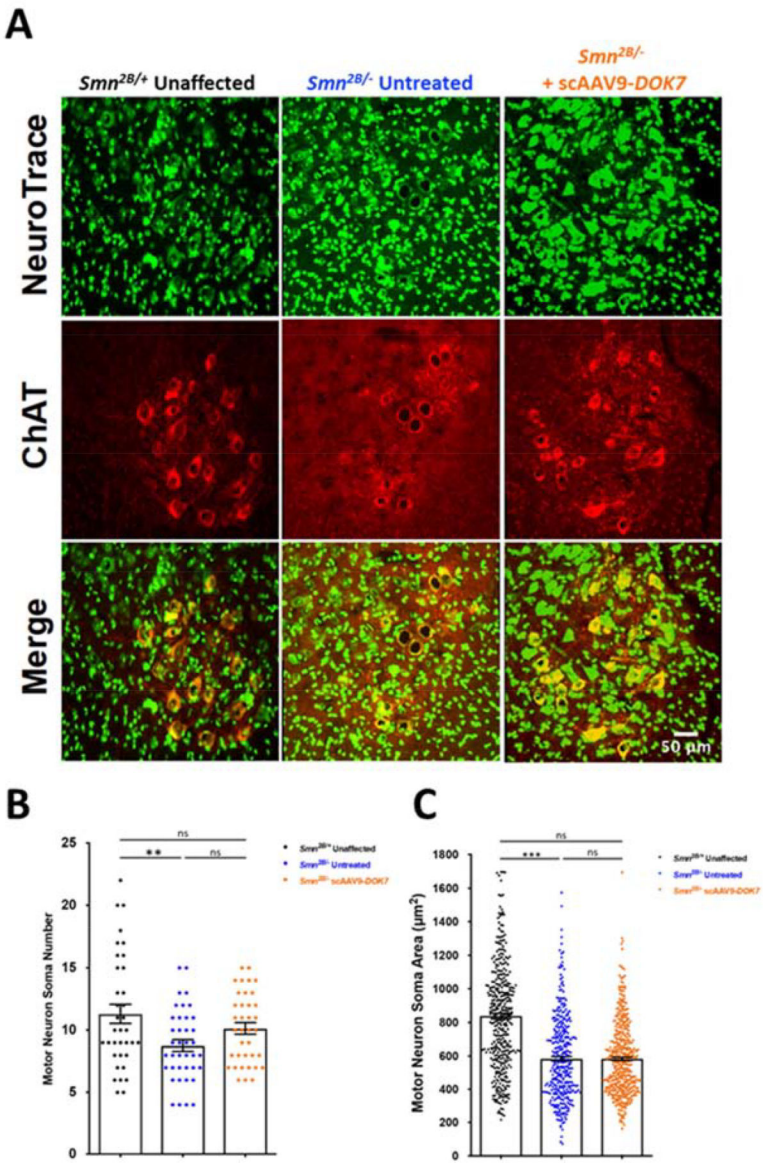

Figure 3: scAAV9-*DOK7* does not improve central defects in *Smn*$^{2B/-}$ mice.

(**A**) Motor neuron soma analyses were performed at P21 (n=3 mice). Representative images of immunofluorescent labelling of ChAT-positive (red) motor neuron soma and NeuroTrace Nissl (green) in the L4-L6 spinal cord (Scale bars = 50 μm). (**B**) Scatter plot representing number of ChAT-positive motor neuron soma in the L4-L6 spinal cord. (**C**) Scatter plot representing cross sectional area of ChAT-positive motor neuron soma in the L4-L6 spinal cord. Bars represent mean ± SEM. Experimental groups were compared using one-way ANOVA with Tukey's multiple comparisons test. (**$P < 0.01$, ***$P < 0.001$, $^{ns}P > 0.05$)

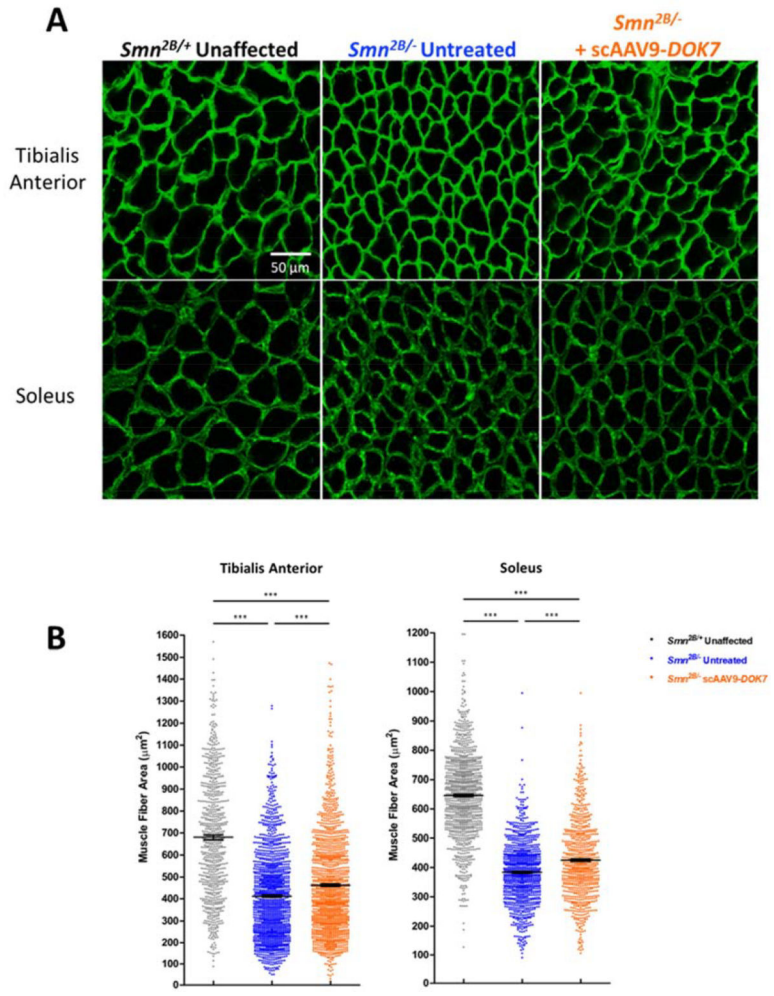

Figure 4: scAAV9-*DOK7* reduces muscle fiber pathology in *Smn*$^{2B/-}$ mice.

Muscle analysis was performed at P17 (n=4 mice). (**A**) Representative images of cross sections of tibialis anterior and soleus muscles dissected on P17. Sections were stained with laminin (green). Images were taken with 40× objective lens (Scale bars = 50 μm). (**B**) Scatter plot representing cross sectional area of TA and SO muscle fibers. Experimental groups were compared using one-way ANOVA with Tukey's multiple comparisons test. (***$P < 0.001$)